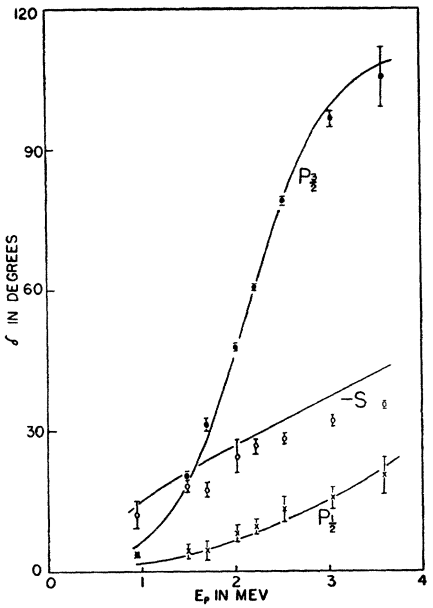

FIG. 1. Phase shifts for $p-\alpha$ scattering as a function of proton bombardment energy.

equal to $-l$ at the nuclear surface. The level shift, Δ, is equal[7] to

$$-\frac{\gamma^2}{a}\left(d\frac{\ln(F_l^2(a)+G_l^2(a))^{\frac{1}{2}}}{d\ln ka}+l\right).$$

Critchfield and Dodder[8] have shown that the $p-\alpha$ differential cross section is consistent with either of two sets of phase shifts, one representing an inverted doublet with an undetermined large splitting, the other corresponding to a regular doublet with a splitting of about one Mev. The points on Fig. 1 represent their values for the phase shifts in the former case, together with their estimate of the probable error. The curves represent the best fit, obtained by trial and error, of Eq. (1) to the points. Corresponding values of the parameters were $a=2.9\times10^{-13}$ cm, $\gamma^2(P_{3/2})=\gamma^2(P_{1/2})=17.6\times10^{-13}$ Mev cm, $E_\lambda(P_{3/2})=3.65$ Mev, and the doublet splitting $E_\lambda(P_{1/2})-E_\lambda(P_{3/2})=5$ Mev. The S-wave curve was calculated using only the potential scattering part of the resonance formula, $\delta_0=-\tan^{-1}[F_0(a)/G_0(a)]$. Effects of high lying levels would be expected to reduce this phase shift in agreement with the experimental results.

The total $n-\alpha$ cross section will equal

$$\sigma_t=2\pi k^{-2}\Sigma_{l,j}(2j+1)\sin^2\delta(l,j), \qquad (2)$$

where $\delta(P_{3/2})$ and $\delta(P_{1/2})$ are calculated from Eq. (1). The points on Fig. 2 are the experimental values of reference 2, while the curve represents the fit of Eq. (2) to the data, using the same values of the parameters, a, γ^2, and the splitting $E_\lambda(P_{1/2})-E_\lambda(P_{3/2})$, as for the $p-\alpha$ analysis. The discrepancy between the data and the curve at 1.2 Mev can be accounted for by an experimental effect discussed in reference 2. The $n-\alpha$ levels are 1.25 Mev lower than the $p-\alpha$ levels, a shift attributable to the difference in coulomb energy. The $n-\alpha$ S-wave phase shifts were calculated by requiring the wave function to have the same logarithmic derivative at the nuclear surface as the $p-\alpha$ S-wave. This leads to a value of about 0.8 barn for the low energy cross section, consistent with reference 2, but in disagreement with the value of 1.45 barns reported by Harris.[9] The sign of the S-wave phase shift is negative,[10] as is the proton phase shift. It seems reasonable to assume that the higher angular momenta phase shifts are negligible. Goldstein[11] has pointed out that this assignment of levels is consistent with the $n-\alpha$ angular distribution and back scattering experiments. For both Li^5 and He^5 the parameters for the $P_{1/2}$ level are somewhat arbitrary.

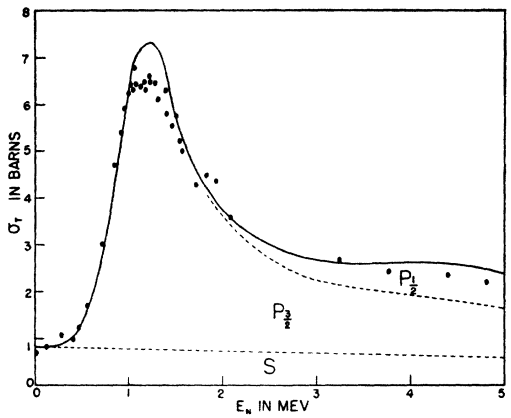

FIG. 2. $n-\alpha$ total cross section as a function of neutron bombardment energy. The dashed lines separate the contributions of the various partial waves.

The value obtained for the reduced width, γ^2, is about equal to $\hbar^2/ma$, where m is the reduced mass of the system. With this value of γ^2 and $|E_\lambda-E|\lesssim\gamma^2/a$, Eq. (1) takes the same form as the result for scattering by a square well of depth E', where $(E'+E_\lambda)^{\frac{1}{2}}(2ma/\hbar^2)^{\frac{1}{2}}=\pi(l+1)$, indicating that the interaction may be represented adequately as a one-body interaction. E' should provide an estimate of the average interaction energy. $E'+E_\lambda$ is equal to 38 Mev for a radius a of 2.9×10^{-13} cm.

In summary, it appears that the data are consistent with the thesis of charge independent forces and the formation of a widely spaced inverted $P_{3/2}-P_{1/2}$ doublet. The doublet splitting of the order of five Mev is much larger than Dancoff's[12] estimate of the effect of tensor forces and may be evidence for the importance of velocity dependent forces,[13] or some other large spin orbit coupling as is postulated for one of the nuclear shell models.[14]

[1] Freier, Lampi, Sleator, and Williams, Phys. Rev. **75**, 1345 (1949).
[2] Bashkin, Petree, and Mooring, Phys. Rev. **82**, 378 (1951).
[3] H. H. Barschall and M. H. Kanner, Phys. Rev. **58**, 590 (1940); T. A. Hall and P. G. Koontz, Phys. Rev. **72**, 196 (1947).
[4] H. Staub and H. Tatel, Phys. Rev. **58**, 820 (1940).
[5] Feshbach, Peaslee, and Weisskopf, Phys. Rev. **71**, 145 (1947); E. P. Wigner and L. Eisenbud, Phys. Rev. **72**, 29 (1947).
[6] These functions were computed with the aid of tables of coulomb wave functions prepared by Bloch, Hull, Broyles, Bouricius, Freeman, and Breit (private communication).
[7] R. G. Thomas, Phys. Rev. **81**, 148 (1951).
[8] C. L. Critchfield and D. C. Dodder, Phys. Rev. **76**, 602 (1949).
[9] S. Harris, Phys. Rev. **79**, 219 (1950).
[10] A. W. McReynolds and R. J. Weiss (private communication).
[11] Herbert Goldstein, Phys. Rev. **79**, 740 (1950).
[12] S. Dancoff, Phys. Rev. **58**, 326 (1940).
[13] C. H. Blanchard and R. Avery, Phys. Rev. **81**, 35 (1951); J. Hughes and K. J. LeCouteur, Proc. Phys. Soc. (London) **63**, 1219 (1950).
[14] M. G. Mayer, Phys. Rev. **75**, 1969 (1949); Haxel, Jensen, and Suess, Phys. Rev. **75**, 1766 (1949).

Emission of the Forbidden Oxygen Lines by Molecular Dissociation

RENÉE HERMAN
Observatoire de Meudon
CHARLES WENIGER
Laboratoire du Grand Electroaimant de Bellevue
AND
LOUIS HERMAN*
Laboratoire de Recherches Physiques, Université de Paris, Paris, France
(Received February 23, 1951)

THE process which occurs in a gas when it is excited by an electrical discharge is often quite complicated. It is not easy to distinguish in the emission spectrum the parts coming from the direct electronic excitation, from the recombination of ions and electrons, and from secondary reactions such as atomic recombination or molecular decomposition.

The radiative ion-electron recombination can be observed in afterglow when the excitation is stopped. In fact, this method is applicable in a limited number of cases, for instance, for rare gases, for nitrogen and gases more or less diluted in a rare gas, and generally for non-electronegative atoms and molecules.

When the production of an atom in a given level is very high, the relative intensity of the emission line can be far from that corresponding to the thermal distribution of atoms in the upper state. This effect is noticeable when the upper level is a metastable one. In this case, intermolecular collisions are frequent and the deactivation is so strong that usually forbidden lines are not observed except under special conditions. The observation of these lines is possible only when the destruction of the atoms in the upper level can be lowered, for instance, by the addition of a rare gas or by compensation by a high production of such metastable atoms in some special way.

The production of forbidden lines by secondary processes is illustrated in Fig. 1 (a and b), in which the atomic levels are shown

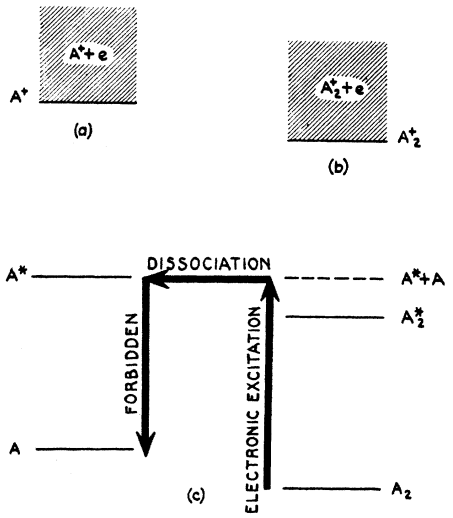

FIG. 1. Illustration of the process of excitation of the forbidden lines 6300 ($^3P_2-^1D_2$) and 6364 ($^3P_1-^1D_2$) of O*I* by dissociation into atoms of the O_2 molecule in the $B^3\Sigma_u^-$ state.

on the left, and the molecular levels on the right. Atomic lines and molecular bands can be excited by electron collisions or can be emitted by ion recombination. Since atoms can associate and molecules can dissociate, an interaction between the two main processes can take place. Two such examples occur in connection with emission of forbidden oxygen lines in the upper part of the atmosphere. The first concerns the red auroral lines 6300A ($^3P_2-^1D_2$) and 6364A ($^3P_1-^1D_2$) of high strength in the light of the high altitude aurora. The second concerns the common green auroral line 5577A ($^1D_2-^1S_0$) which is the main part of the emission of the night sky and aurora.

The process of electronic excitation, we believe, may be illustrated by the pattern indicated in heavy lines in Fig. 1(c).

In the case of the red aurora lines the upper excited molecular state is $B^3\Sigma_u^-$. This state is stable and the corresponding transition gives the Schumann-Runge bands $B^3\Sigma_u^-\rightarrow X^3\Sigma_g^-$ in absorption and in emission. To reach the dissociation of the upper state into two atoms $O(^3P)+O(^1D_2)$, a considerable development of this band system must be obtained. In fact, this is observed together with an important relative enhancement of the 6300 and 6364 lines in pure oxygen at atmospheric pressure (Fig. 2).

The second example concerns the emission of a mixture of a rare gas like xenon or argon and a small amount of oxygen. The green emission observed in the direct discharge and in afterglow is composed of two parts, the auroral line 5577A ($^1D_2-^1S_0$), and a

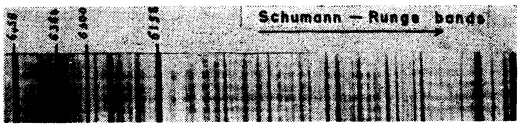

FIG. 2. Emission spectrum of pure oxygen at atmospheric pressure. The forbidden red auroral lines 6300 and 6364 and the Schumann-Runge bands are particularly strong.

quasi-continuous molecular spectrum mainly on the short wavelength side of the line.[1,2] Here, the lower and the upper molecular states have a very low dissociation energy.

In a mixture of oxygen and xenon, one observes a well-developed system of bands which is relatively easy to identify. On the contrary, in the case of argon containing traces of oxygen, the vibrational bands are most confused and upon examination under low dispersion the emission appears purely continuous.[3-5]

We have nevertheless succeeded in resolving the vibrational structure in the continuous background on the two sides of the auroral line. The complete system is degraded towards short wavelengths, and the intensity diminishes rapidly. At a distance from the auroral line, the bands have been photographed with lower dispersion and show definite fluctuations of intensity degraded to the red. The apparent heads of these bands are located approximately at 5487A, 5529A, and 5555A.

On the other hand, a somewhat complex structure appears near the green line. We attribute this to vibrational bands of the electronic transition $AO(^1S_0;{}^1S_0)\rightarrow AO(^1S_0;{}^1D_2)$. A tentative vibrational classification of the most intense bands[6] is shown in Table I.

For the XO molecule the vibrational frequency ω' is nearly 10 times and ω'' 20 times greater than for the AO molecule; the

TABLE I. Wave numbers of the green band system observed near the forbidden oxygen line 5577 ($^1D_2-^1S_0$) of O *I* in a mixture of argon and oxygen. v' and v'' are the vibrational quantum numbers of the upper and the lower states.

v' \ v''	0	1	2	3	4	5	6	7
0	17939	17915						
1	17956	17933						
2		17948						
3		17962	17937					
4			17953					
5				17945	17920			
6					17936			
7				17976		17928	17910	
8					17967	17945	17926	17905
9					17981			
10							17958	

latter is thus much less stable since $\omega''>\omega'$, and the individual bands will be degraded to the red. On the microphotometer traces we recognized no degradation as the bands strongly overlap.

It is probable that the bands 5487A, 5529A, and 5555A are likewise capable of resolution. To resolve them, it will be necessary to employ a spectrograph which is (at the same time) of higher speed and of greater dispersion than the one at our disposal.

The spectral composition of this green emission is the same in afterglow and in the direct discharge. Thus, the green auroral line seems closely connected with the quasi-continuous part. On the other hand, the remaining permitted and forbidden O*I* lines are very faint if not absent, and it is hardly to be supposed that there exists a low electronic excitation of the diluted atomic oxygen.

* Temporarily at the Geophysical Institute, College, Alaska.

[1] Kenty, Aicher, Noel, Poritsky, and Paolino, Phys. Rev. **69**, 36 (1946).
[2] R. Herman, Compt. rend. **222**, 492 (1946).
[3] L. Herman and R. Herman, Ann. Geophys. **I**, 165 (1944).
[4] Vegard, and Kvifte, Nature **162**, 967 (1948).
[5] Jenkins, Bowtell, and Strong, Nature **163**, 401 (1949).
[6] K. G. Emeleus and N. D. Sayers, University of Belfast, found a partially similar structure in their independent work on the same band system (private communication).

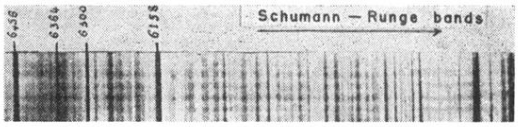

FIG. 2. Emission spectrum of pure oxygen at atmospheric pressure. The forbidden red auroral lines 6300 and 6364 and the Schumann-Runge bands are particularly strong.